

SUPPORTING INFORMATION: MODEL DEVELOPMENT

Multiplexing engineered receptors for multiparametric evaluation of environmental ligands

Rachel M. Hartfield*¹, Kelly A. Schwarz*¹, Joseph J. Muldoon*^{1,2}, Neda Bagheri^{1,2,3,4,5,6},
Joshua N. Leonard^{1,2,3,4,5}

*These authors contributed equally to this work

¹Department of Chemical and Biological Engineering, Northwestern University, Evanston, Illinois 60208, United States

²Interdisciplinary Biological Sciences Program, Northwestern University, Evanston, Illinois 60208, United States

³Center for Synthetic Biology, Northwestern University, Evanston, Illinois 60208, United States

⁴Chemistry of Life Processes Institute, Northwestern University, Evanston, Illinois 60208, United States

⁵Member, Robert H. Lurie Comprehensive Cancer Center, Northwestern University, Evanston, Illinois 60208, United States

⁶Northwestern Institute on Complex Systems, Northwestern University, Evanston, Illinois 60208, United States

Correspondence to: Joshua N. Leonard, j-leonard@northwestern.edu

Contents

<u>Topic</u>	<u>Page</u>
I. Overview	3
II. Intercellular variation model	
A. Experiment	4
B. Model development	4
C. Model analysis	4
III. Logic gate promoter model	
A. Experiment	6
B. Model development	9
C. Model analysis	11
IV. MESA model	
A. Variables	15
B. Parameter estimates	15
C. Reactions	16
D. Fixed parameters	17
E. Conditions	18
F. TFs and reporters	19
V. Model predictions	
A. Dosing	24
B. Time points	27
C. Promoters	28
VI. References	29

I. OVERVIEW

This supporting information file describes the development, calibration, and analysis of the computational model for multiplexed MESA signaling and hybrid promoter activity, summarized in **Figure M1**. We (1) present an approach to account for intercellular variation that arises from differences such as in transfection, transcription, and translation, (2) quantify the effect of variation on reporter expression, and (3) demonstrate how variation affects the experimental characterization and implementation of genetic circuits. Incorporating this variation explicitly into the model calibration and analysis enabled us to better explain experimental data, infer outcomes for individual cells, and predict strategies for receptor engineering and promoter engineering to improve AND gate performance.

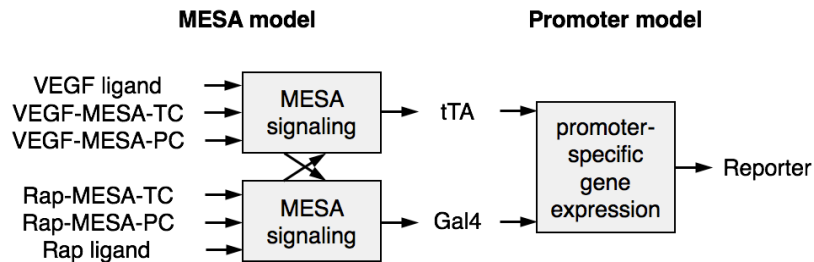


Figure M1: Model overview. In the MESA model, target chain (TC) and protease chain (PC) proteins are expressed from plasmids that can be transfected at different doses, and transported via exocytosis to the cell surface. There are two MESA receptors—one senses VEGF and the other rapamycin (Rap)—which ligand-inducibly signal independently, but can exhibit crosstalk in non-ligand mediated signaling. Downstream of the receptors are the hybrid promoters H1 and H2, which are regulated by the transcription factors (TFs) tTA and Gal4. Each TF can be expressed either on a MESA target chain and potentially released by receptor signaling, or in constitutively soluble form that bypasses the requirement for receptor signaling. Promoter activity is characterized by measuring the expression (fluorescence) of a promoter-driven reporter protein.

II. INTERCELLULAR VARIATION MODEL

A. Experiment

To generate data for informing a model of intercellular variation, HEK293FT cells were cotransfected with three plasmids that each express a fluorescent protein constitutively (colors: red, green, blue). Cells were gated for live, singlets, and blue+ using flow cytometry. Post-gating distributions of red and green are analogous to post-gating distributions in other experiments that involve functional plasmids for MESA, soluble TFs, and inducible reporters. The marginal distribution of each fluorescent protein was bimodal on a \log_{10} -scaled axis, and this distribution showed a wide range of expression across the population of cells (**Figure M2a**). For the purposes of this model, we describe variability in plasmid dose as the main driver of inherent intercellular variation, although in fact such “inherent” variation depends on differences in transcription and translation rates between cells as well. Green and red fluorescence were correlated ($r \sim 0.8$ on linear-scaled axes; $r \sim 0.9$ on \log_{10} -scaled axes), suggesting that if a cell received a low amount of one plasmid (and exhibited low expression of the corresponding fluorescent marker), then that cell likely received low amounts of other plasmids, and vice versa for cells that receive high amounts of plasmids.

B. Model development

The marginal distribution for green fluorescence was estimated by formulating and training a bimodal log-scaled Gaussian mixture model (GMM) on the data (**Figure M2b**). A candidate *in silico* population was produced by randomly co-sampling n values (one per plasmid) 200 times (one for each cell) from the GMM. The joint distribution of the resulting population (Z) can be represented as a $200 \times n$ matrix. This population size was chosen based on an empirical assessment for balancing two objectives: (1) have sufficient cells to resemble the kernel density estimate of the target marginal, and (2) avoid requiring excessive computational expense in subsequent simulations for parameter estimation. Since the GMM is bimodal and Gaussian, random sampling was conducted using a multivariate normal random number generator. The random numbers were transformed based on the mean and standard deviation (S.D.) for each of the two GMM modes. Since $\sim 40\%$ of the experimental population was estimated to be in the lower mode, 80 cells were drawn from the mean and S.D. of the lower mode and 120 from the mean and S.D. of the upper mode.

The covariance matrix ($n \times n$) for the candidate population was calculated. If the pairwise correlation in each entry (other than entries along the diagonal) was within a user-specified window ($0.77 < r < 0.83$, which approximates the experimental correlation), then the candidate was accepted. However, if at least one entry was outside of the window, then the procedure was repeated by generating new candidates until one was accepted. For $n = 5$ plasmids, the number of candidates that were tested before one was accepted varied between $\sim 10^4$ to 10^6 . The resulting population exhibited the expected marginal and joint distributions. Each linear-scaled distribution was normalized to a mean of one arbitrary unit of plasmid that a cell receives per microgram of plasmid transfected in a well of a 24-well plate (a.u. μg^{-1}), so that in subsequent model simulations the transfection dose (μg) could be specified via a scalar multiplier to the dose of each plasmid.

C. Model analysis

The intercellular variation model attributes population variability to two sources—1) inherent intercellular variation including the varied amounts of plasmids received in the transfection procedure, and 2) the cotransfection of multiple plasmids—which contribute their effects as orthogonal vectors. Principal component analysis on Z showed that, for two plasmids, cotransfection explained 10% of the variance and intercellular variation explained 90%. For five plasmids, the percentage explained by intercellular variation decreased modestly to 84%. Therefore, if the number of plasmids were decreased by cloning multiple genes onto the same plasmid, even if the total number of plasmids decreased substantially, this strategy would be predicted to eliminate the minor source and not the major source.

Another prediction is that for a genetic circuit in which variance in the transfection procedure propagates nonlinearly to reporter expression, each plasmid’s variation over several orders of magnitude could be magnified multiplicatively. Additionally, the covariance between cotransfected plasmids could exacerbate the incidence of lower and upper extremes in reporter expression, because cells that receive low or high amounts of one plasmid are likely to receive similar amounts respectively of other cotransfected plasmids.

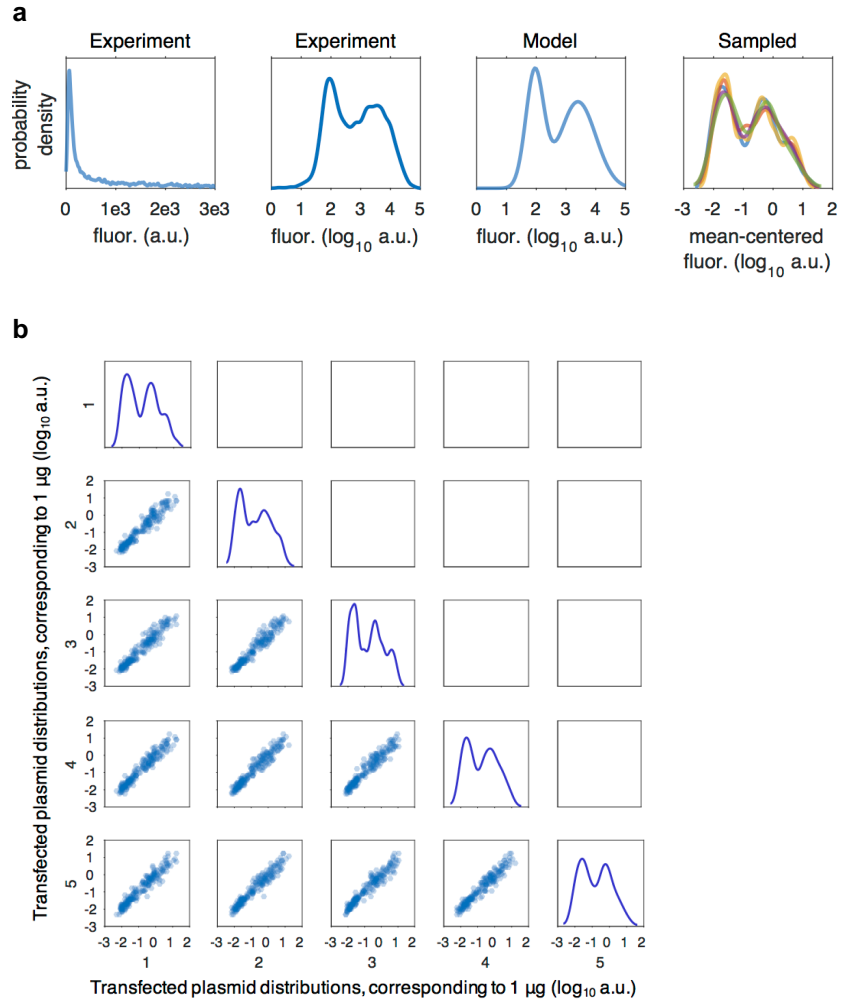


Figure M2: Transfection model. (a) The marginal distribution of a transfected plasmid was modeled using a bimodal Gaussian: $f = c \cdot N(\mu_1, \sigma_1) + (1 - c) \cdot N(\mu_2, \sigma_2)$, where each μ is a mean, each σ is a standard deviation, and c is a value between zero and one. Parameters were estimated based on experimental data: $c = 0.4$, $\mu_1 = 1.95$, $\sigma_1 = 0.3$, $\mu_2 = 3.4$, $\sigma_2 = 0.6$. The linearly-scaled distribution for each plasmid in the distribution was mean-centered to one (equal to zero on the \log_{10} -scaled x-axis). The right-most panel shows the distributions of five plasmids that were co-sampled to produce a 200-cell *in silico* population. **(b)** The five plots along the diagonal show the marginal distribution for each plasmid in the *in silico* population, and the y-axis for these plots is probability density. The other plots show the joint distribution (200 cells) for each pair of different plasmids.

III. LOGIC GATE PROMOTER MODEL

A. Experiment

We observed by flow cytometry that most cells transfected with plasmids for the TFs and reporter expressed the reporter protein at fluorescence levels comparable to cells that were transfected with reporter only. Across experiments, a small subpopulation was distinguishably “ON”. To describe this heterogeneity, we define several metrics, which can be applied to both the experiments and simulations (**Figure M3**).

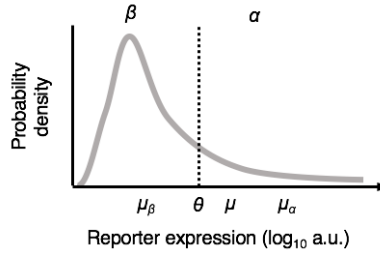


Figure M3: Metrics for heterogeneous reporter expression. Metrics are: θ : Threshold for ON vs. OFF. α : Proportion of ON cells. β : Proportion of OFF cells. μ : Population mean. μ_α : ON subpopulation mean. μ_β : OFF subpopulation mean.

The percentages of ON cells in experiments corresponding to figures in the main text (indicated in the parentheses) are shown below, rounded to the nearest tenth of a percent (**Table M1a-l**).

Table M1a. Two soluble TFs with H1 promoter (for Figure 1d).

		Soluble tTA (μg)					
		Dose	0	0.005	0.05	0.10	0.50
Soluble Gal4 (μg)	0	<0.1	<0.1	0.6	1.3	3.1	
	0.005	0.4	0.4	8.0	2.4	11.4	
	0.05	2.6	3.0	14.3	10.9	11.4	
	0.10	7.2	7.5	18.1	16.6	17.8	
	0.50	9.2	13.6	18.1	17.3	16.2	

Table M1b. Two soluble TFs with H2 promoter (for Figure 1d).

		Soluble tTA (μg)					
		Dose	0	0.005	0.05	0.10	0.50
Soluble Gal4 (μg)	0	0.1	<0.1	0.1	0.1	0.8	
	0.005	0.1	0.2	0.8	1.6	2.1	
	0.05	1.3	1.2	5.8	5.9	10.3	
	0.10	1.9	2.6	10.6	10.0	17.5	
	0.50	4.0	5.3	9.2	8.5	16.0	

Table M1c. Rap-MESA and soluble tTA with H1 promoter (for Figure 2a).

		Rap-TC (μg)							
		Dose	0	0.005	0.05	0.10	0.50	1.0	2.0
Rap-PC (μg)	0	0	0.1	0.1	0.4	0.8	n/a	0.1	
	0.005	0.1	0.2	0.2	0.7	1.2	1.7	1.5	
	0.05	0.2	n/a	0	1.0	1.6	1.6	1.3	
	0.10	0.1	n/a	n/a	0.7	1.9	1.4	1.6	
	0.50	0.1	n/a	n/a	n/a	1.8	1.9	1.6	

Table M1d. Rap-MESA and soluble tTA with H1 promoter and Rap (for Figure 2a).

		Rap-TC (μg)						
Dose		0	0.005	0.05	0.10	0.50	1.0	2.0
Rap-PC (μg)	0	0	0.1	0.2	0.2	0.6	n/a	0.1
	0.005	0.1	0.2	0.2	0.6	0.9	1.2	1.3
	0.05	0.1	n/a	<0.1	1.1	0.9	1.1	1.1
	0.10	0.1	n/a	n/a	1.2	1.7	1.2	0.9
	0.50	0.1	n/a	n/a	n/a	1.6	1.7	1.2

Table M1e. VEGF-MESA and soluble Gal4 with H1 promoter (for Figure 2a).

		VEGF-TC (μg)						
Dose		0	0.005	0.05	0.10	0.50	1.0	2.0
VEGF-PC (μg)	0	0	0.9	1.1	0.1	1.2	n/a	0
	0.005	0.7	1.5	1.1	0.1	1.8	7.6	9.2
	0.05	1.0	n/a	2.0	0.1	1.8	8.5	8.9
	0.10	0.9	n/a	n/a	0.2	2.0	9.8	13.2
	0.50	1.2	n/a	n/a	n/a	2.7	14.1	11.3

Table M1f. VEGF-MESA and soluble Gal4 with H1 promoter and VEGF (for Figure 2a).

		VEGF-TC (μg)						
Dose		0	0.005	0.05	0.10	0.50	1.0	2.0
VEGF-PC (μg)	0	0	1.0	1.0	1.1	1.0	n/a	0.1
	0.005	0.7	1.4	1.1	1.2	1.4	8.0	10.4
	0.05	0.7	n/a	2.0	1.5	2.1	8.3	9.3
	0.10	0.9	n/a	n/a	1.5	1.7	9.7	11.0
	0.50	1.0	n/a	n/a	n/a	2.8	12.3	10.8

Table M1g. Rap-MESA and soluble tTA with H2 promoter (for Figure 2a).

		Rap-TC (μg)						
Dose		0	0.005	0.05	0.10	0.50	1.0	2.0
Rap-PC (μg)	0	0.2	0.1	<0.1	0.3	0.7	4.9	2.7
	0.005	0.3	0.3	1.3	1.4	4.9	6.6	5.0
	0.05	0.1	n/a	1.2	2.7	4.4	7.3	4.8
	0.10	<0.1	n/a	n/a	3.6	4.2	6.7	6.0
	0.50	<0.1	n/a	n/a	n/a	4.8	6.2	4.4

Table M1h. Rap-MESA and soluble tTA with H2 promoter and Rap (for Figure 2a).

		Rap-TC (μg)						
Dose		0	0.005	0.05	0.10	0.50	1.0	2.0
Rap-PC (μg)	0	n/a	n/a	n/a	n/a	n/a	n/a	n/a
	0.005	n/a	0.5	1.0	1.4	3.8	3.3	4.7
	0.05	n/a	n/a	4.3	4.2	3.4	3.6	6.1
	0.10	n/a	n/a	n/a	1.4	2.6	4.2	6.4
	0.50	n/a	n/a	n/a	n/a	4.3	3.1	5.8

Table M1i. VEGF-MESA and soluble Gal4 with H2 promoter (for Figure 2a).

		VEGF-TC (μg)						
VEGF-PC (μg)	Dose	0	0.005	0.05	0.10	0.50	1.0	2.0
	0	0.2	7.4	0.7	12.3	11.7	15.6	13.3
	0.005	12.8	11.3	10.4	13.8	14.4	15.5	14.3
	0.05	9.5	n/a	11.4	12.1	13.0	13.9	15.0
	0.10	9.5	n/a	n/a	12.8	17.8	14.9	17.2
	0.50	10.4	n/a	n/a	n/a	13.0	20.7	6.8

Table M1j. VEGF-MESA and soluble Gal4 with H2 promoter and VEGF (for Figure 2a).

		VEGF-TC (μg)							
VEGF-PC (μg)	Dose	0	0.005	0.05	0.10	0.50	1.0	2.0	
	0	n/a	n/a	n/a	n/a	n/a	n/a	n/a	n/a
	0.005	n/a	9.9	11.7	10.1	11.0	12.7	16.0	
	0.05	n/a	n/a	11.9	10.4	13.6	12.8	16.3	
	0.10	n/a	n/a	n/a	11.0	11.6	12.7	16.9	
	0.50	n/a	n/a	n/a	n/a	12.3	19.1	7.7	

Table M1k. Two MESA with H1 promoter, with and without each ligand (for Figure 2b).

Ligands	VEGF	-	+	-	+
	Rap	-	-	+	+
VEGF-PC (μg)	0.005	0.3	0.5	0.4	0.7
	0.05	0.5	0.5	0.7	1.0
	0.10	0.4	0.3	1.4	2.1
	0.50	0.4	0.3	1.0	1.2

Table M1l. Two MESA with H2 promoter, with and without each ligand (for Figure 2b).

Ligands	VEGF	-	+	-	+
	Rap	-	-	+	+
VEGF-PC (μg)	0.005	0.1	<0.1	0.1	<0.1
	0.05	0.1	<0.1	<0.1	0.1
	0.10	<0.1	<0.1	0.1	<0.1
	0.50	<0.1	<0.1	0.1	<0.1

B. Model development

An ODE model for synergistic transcriptional activation of the hybrid promoters H1 and H2 by two soluble TFs tTA and Gal4 was formulated (**Tables M2 and M3**). Included in the term for transcription of the reporter is fractional activation (f), which is a unitless quantity between [0, 1) for promoter activity. In the tables, units are: concentration in arbitrary units (U), time in hours (h), or not applicable (N/A).

$$f = \frac{w_T \cdot [\text{tTA}] + w_G \cdot [\text{Gal4}] + w_{TG} \cdot [\text{tTA}] \cdot [\text{Gal4}]}{1 + w_T \cdot [\text{tTA}] + w_G \cdot [\text{Gal4}] + w_{TG} \cdot [\text{tTA}] \cdot [\text{Gal4}]}$$

Dividing the effect of both TFs together by the responsiveness to each individual TF yields a metric for synergy: $\rho = w_{TG} / (w_T \cdot w_G)$ in units of U^{-1} .

Table M2: Parameters for the promoter model.

Parameters	Values	Units	Descriptions
$z1, z2, z3$	varies	N/A	Varied amounts of each plasmid from transfection
k_{syn}	1	$U h^{-1}$	Constitutive TF production (arbitrary scalar)
$dF1$	varies	N/A	Transfection dose of soluble tTA plasmid
$dF2$	varies	N/A	Transfection dose of soluble Gal4 plasmid
k_{degF1}, k_{degF2}	2	h^{-1}	Degradation of each soluble TF(di Bernardo et al., 2011)
k_{tx}	1	$U h^{-1}$	Max. rate of transcription of reporter (arbitrary scalar)
k_{tl}	1	h^{-1}	Translation of reporter (arbitrary scalar)
$k_{degRepR}$	2.3	h^{-1}	Degradation of reporter RNA(Siciliano et al., 2011)
$k_{degRepP}$	0.054	h^{-1}	Degradation of reporter protein(Siciliano et al., 2011)

Table M3: System of ODEs for the promoter model.

#	Variables	ODEs	Descriptions of reactions
1	F1 (tTA)	$z1 * ksyn * dF1$ - $kdegF1 * [F1]$	Production TF degradation
2	F2 (Gal4)	$z2 * ksyn * dF2$ - $kdegF2 * [F2]$	Production TF degradation
3	H1 RNA	$z3 * ktx * f_1([F1], [F2])$ - $kdegRepR * [H1RNA]$	Transcription Reporter RNA degradation
4	H1 protein	$kt1 * [H1RNA]$ - $kdegRepP * [H1Protein]$	Translation Reporter protein degradation
5	H2 RNA	$th3 * ktx * f_2([F1], [F2])$ - $kdegRepR * [H2RNA]$	Transcription Reporter RNA degradation
6	H2 protein	$kt1 * [H2RNA]$ - $kdegRepP * [H2Protein]$	Translation Reporter protein degradation

After calibration of the 200-cell *in silico* population to experimental mean averages (μ) for combinatorial doses of each plasmid using high-dimensional parameter sweeps, multi-objective optimization, and a genetic algorithm (**Table M4**), the model could also accurately account for trends in α and μ_α (Figure 3b, main text). For each promoter, the mean (μ) and proportion of ON cells (α) were similarly and highly correlated (Pearson correlation coefficient, $r \sim 0.97$) in experiments and in simulations. The results show that while each metric describes a feature of population variability, the mean is a sufficient metric for model calibration.

Table M4: Fitted parameters for transcriptional regulation in the promoter model.

#	Parameter	Estimate*	Units	Description
1	w_{H1_T}	$8.594 * 10^{-3}$	N/A	tTA on promoter H1
2	w_{H1_G}	$2.501 * 10^{-1}$	N/A	Gal4 on promoter H1
3	w_{H1_TG}	5.834	U^{-1}	tTA and Gal4 together on promoter H1
4	w_{H2_T}	$1.368 * 10^{-3}$	N/A	tTA on promoter H2
5	w_{H2_G}	$4.563 * 10^{-2}$	N/A	Gal4 on promoter H2
6	w_{H2_TG}	3.561	U^{-1}	tTA and Gal4 together on promoter H2

*We note that the term for fractional activation in model simulations involved the following scalar multiplications to each transcriptional activation parameter:

w_{H1_T} and w_{H1_G} were each multiplied by 2 (for $kdegF1$)
 w_{H2_T} and w_{H2_G} were each multiplied by 2 (for $kdegF2$)
 w_{H1_TG} and w_{H2_TG} were each multiplied by 4 (for $kdegF1 * kdegF2$)

C. Model analysis

Leveraging the model, we sought to analyze outcomes for the population mean compared to individual cells. The model showed that for all plasmid dose combinations, reporter expression for the population mean was greater than that of a cell receiving the mean amounts of transfected plasmids (**Figure M4a**). Cells that received large amounts of plasmids showed much higher than average activity, which can be explained in part by TF synergy at the promoters. An implication is that characterization of the logic gate promoters—and perhaps synthetic genetic circuits in mammalian cells more broadly—may be driven largely by a subpopulation of outlier cells. Therefore, we propose that by facilitating the high-dimensional *mapping* from plasmid-transfection space onto distinct cellular outcomes, a model-guided single-cell analysis may elucidate genetic circuit behaviors more precisely.

At low plasmid doses, the population mean resembles the mean-transfected cell. However, there are no cells that resemble the mean across the dose-response landscape. At low doses, the mean resembles the ~60th percentile transfected cell (near the mean-transfected), and at high doses it resembles the ~75th percentile. Therefore, the mean is biased in that it overestimates promoter responsiveness to increased TF dose (and conversely, underestimates responsiveness to decreased dose). The model predicts that for this reason, when increasing TF doses from 0.02 μg to 0.5 μg for both TF plasmids (from the lower left heatmap corner to the upper right corner) the change in population mean reporter output exceeds that of reporter output in the mean cell by 1.9-fold for H1 and by 1.5-fold for H2.

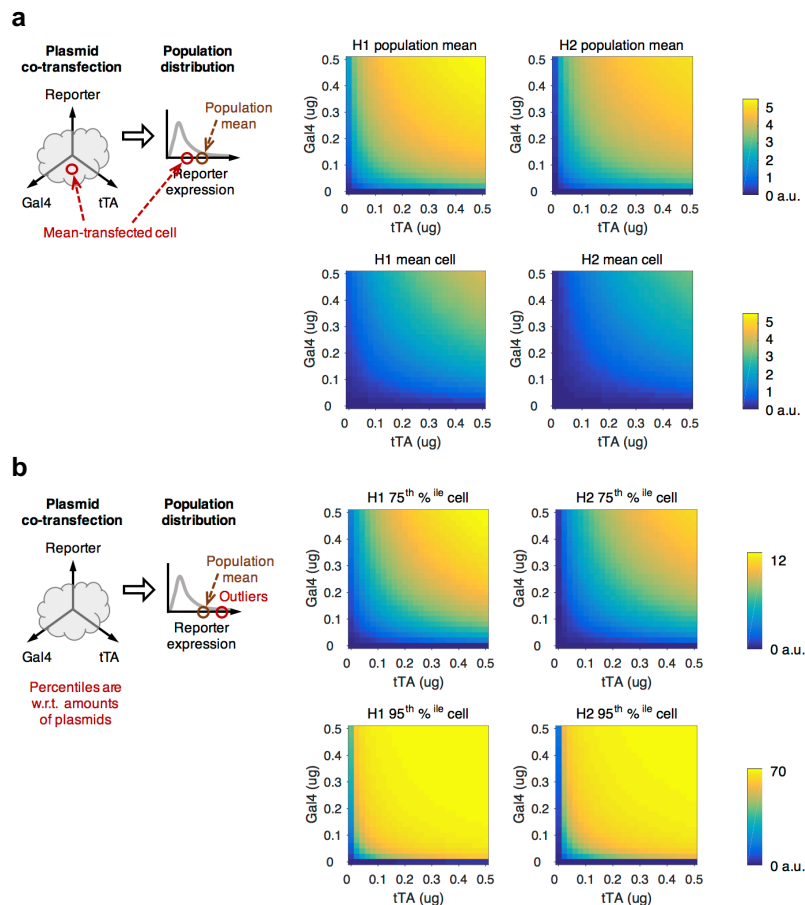


Figure M4: Predicted reporter expression. (a) Reporter expression for the population mean is greater than that of a cell that receives the mean amounts of transfected plasmids. (Due to the right-skewed distribution of intercellular variation, the latter occurs at the 62nd percentile). Axis units are the dose for each TF (μg) that corresponds to the amount of plasmid (a.u.) received by a cell. (b) Cells that receive large amounts of plasmids will have much higher than average promoter activity.

Within an experiment, the amount of each plasmid that a cell receives is correlated: a cell that receives a large amount of one plasmid is likely to receive a similarly high amount of each other plasmid. We expect this correlation should hold across transfection doses. Therefore, although the reporter plasmid dose is consistent across experiments, the amount received by cells within a population still varies, and cells that receive a higher than average amount of TF plasmid also receive a higher than average amount of reporter plasmid (**Figure M4b**). The model explains that for this reason, it is possible to overestimate the fundamental range of promoter activity during the process of promoter characterization. We therefore posit that any experiments that involve the transfection of a reporter plasmid to measure the activity of a genetic component may be susceptible to this issue.

To examine this apparent phenomenon of overestimating promoter activity, a hypothetical scenario was tested in which transfected cells were artificially uniform in the reporter plasmid while two TFs varied as they would normally. Conceptually, one way to visualize this scenario is a two-dimensional cross-section through a three-dimensional *cone of cotransfection* (**Figure M5**; cartoon). (Since the plane of the cross-section is parallel to the plane of the two TF axes, the orientation of the cross-section is slanted relative to the cone's radial axis.) The analysis was conducted across the TF dose landscape as in Figure M4, and shows that for high plasmid doses (Figure M5; upper right corner in heatmaps), cells at the 95th transfection percentile express near-saturating levels of reporter. Therefore, high absolute reporter expression in the upper outlier cells is attributable in part to large amounts of reporter plasmid, rather than only TF activity. Since the level at which saturating reporter expression occurs should scale with the amount of reporter plasmid in a cell, we predict that the limiting factor for fluorescence at high TF doses is the amount of reporter plasmid. As a result, many cells saturate, but at different fluorescence levels. We note that since the reporter plasmid dose is constant across experiments, the highest possible saturation is constant regardless of TF doses, although at high TF doses there would be more cells that approach the highest possible saturation. Additionally, we anticipate that since many effects of intercellular variation are related to amounts of plasmids received by cells in a transfection, the caveats described here for interpreting experimental results may be alleviated by introducing components via stable genomic integration.

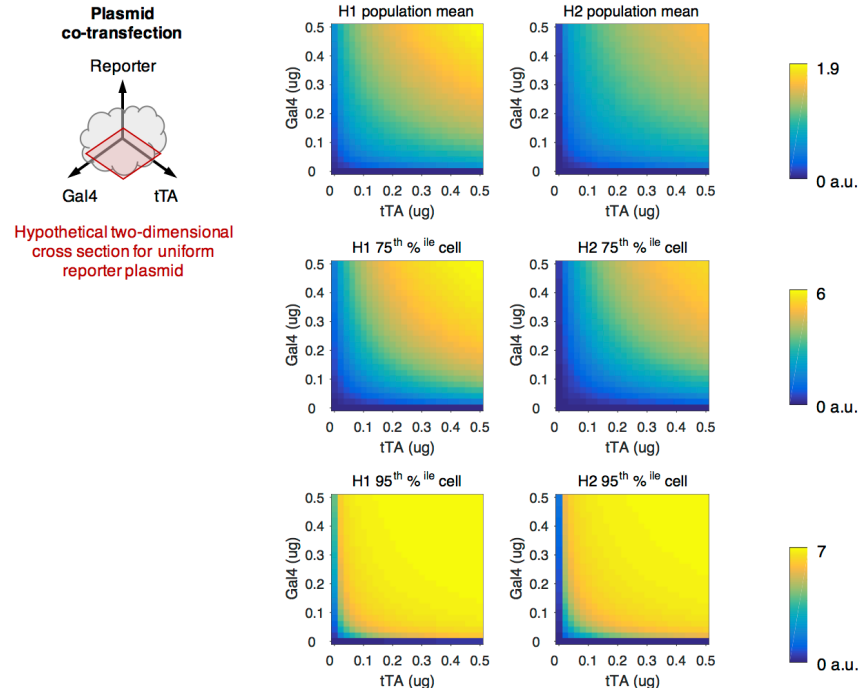


Figure M5: Hypothetical reporter expression, for a uniform amount of transfected reporter plasmid. At high TF doses, the cross-sectional 75th percentile is nearly equal to the cross-sectional 95th, whereas in the non-cross-sectional cases (Figure M4) the outcomes differ. Differences are due to the correlation between cotransfection plasmids. (The mean-transfected cell in Figure M4 is equivalent in the cross-section analysis, and is not duplicated here.)

To assess whether the method for generating *in silico* populations gave similar outcomes across runs, the co-sampling procedure was repeated (**Figure M6**). We observed that joint and marginal distributions were indeed robust across runs for the given population size (200 cells) and number of plasmids ($n = 5$).

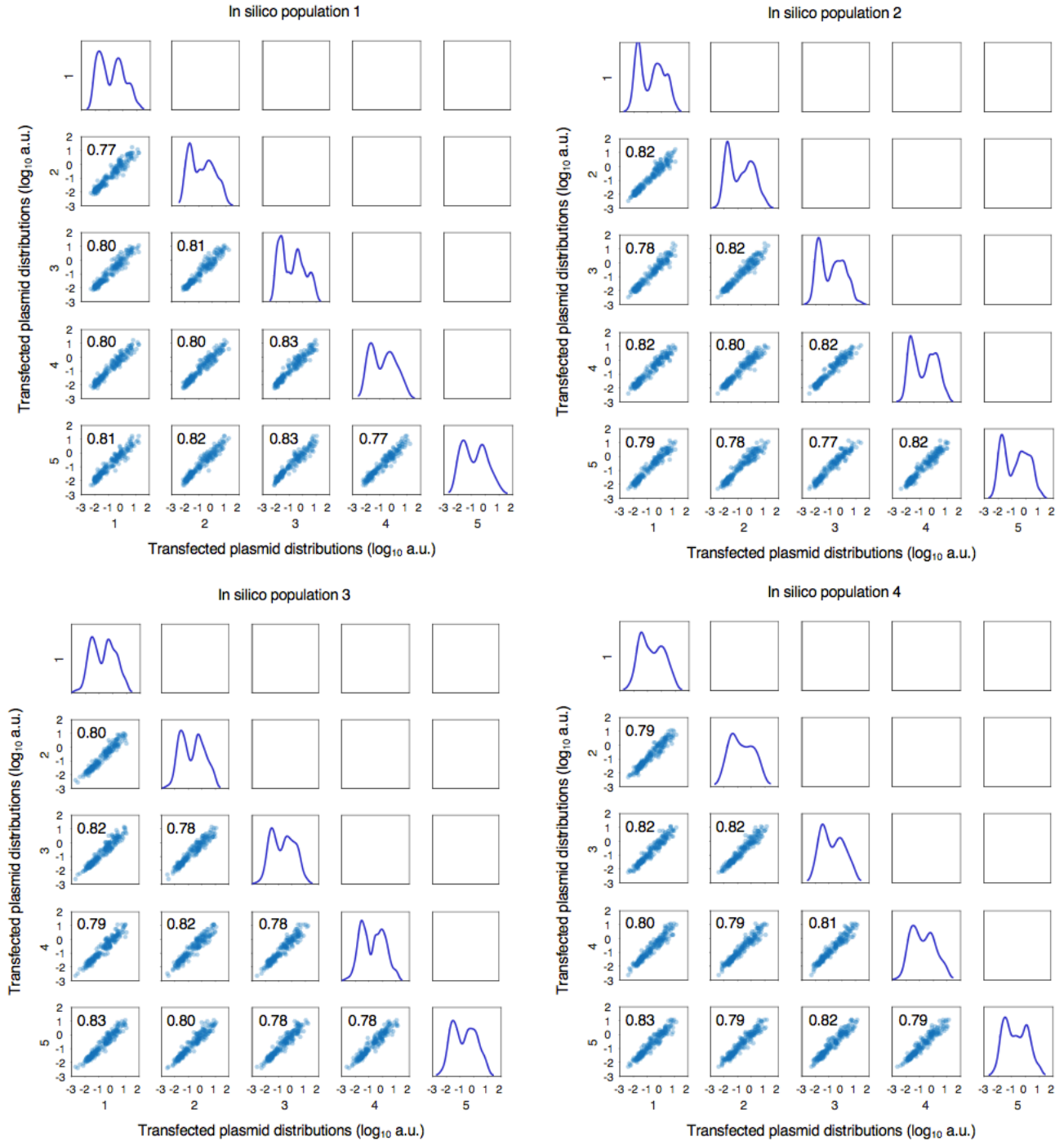


Figure M6: Example *in silico* populations. Marginal distributions, joint distributions, and pairwise correlations for the five plasmids in each of the four separately generated *in silico* populations. The Pearson correlation r for each comparison was determined using linearly scaled axes. (If these values, around 0.8, are instead determined based on \log_{10} -scaled axes, they are around 0.9.) Population #1 is the original one, and was carried forward and used in the MESA model. Populations #2-4 are additional examples.

To assess whether predicted TF dose landscapes were similar across distinctly generated populations, we conducted a similar analysis as in Figure M4 to visualize the mean reporter expression for each of the four populations in Figure M6 (**Figure M7**). Consistent with the observed similarity in transfection distributions across populations, heatmap outcomes were insensitive to the choice of population.

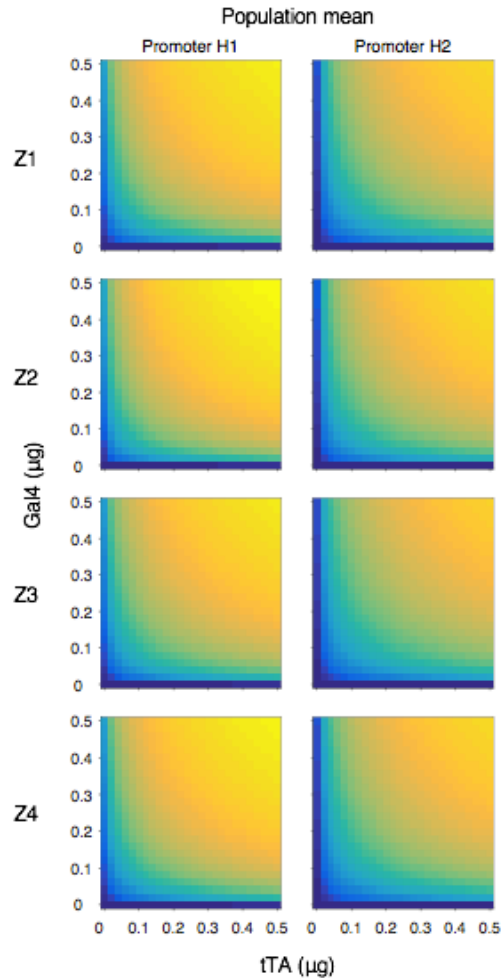


Figure M7: Predicted TF dose landscape is robust to the choice of *in silico* population. The TF dose landscapes of reporter expression (population mean) for promoters H1 and H2 are essentially identical.

IV. MESA MODEL

An ODE model for multiplexed MESA signaling was formulated to account for the reaction mechanism. Several models that differ in mechanistic granularity and in the representation of the mechanism were developed and assessed prior to arriving at a final version. After formulation, the model was calibrated to data from experiments with promoters H1 and H2. Calibration proceeded in two stages: 1) three parameters were fitted using no-ligand data, yielding a family of parameter sets that fit the data similarly; and 2) the remaining three parameters were fitted using data with ligand(s), to arrive at a final parameter set. Fitting was conducted using high-dimensional sweeps (as opposed to, e.g., gradient search) using a Sobol sequence (Sobol, 1976), followed by a window-based multi-objective optimization in which multiple user-specified conditions, based on a subset of salient data, needed to be satisfied for a parameter set to be accepted (as opposed to, e.g., least squares optimization). A custom script for a genetic algorithm was run for several (<20) generations of simulation, scoring, culling, repopulation, and mutation, until no substantial further improvements were observed in the fit to the data.

A. Variables

Variables have initial values of 0 arbitrary units (a.u.). Simulations begin at the time of plasmid transfection (0 h), account for ligand treatment if applicable (12 h), and end at the corresponding experimental time point for flow cytometry (36 h). The model is specified in accompanying MATLAB files. There are up to 11 variables per MESA per cellular compartment (**Table M5**). For Rap-MESA, due to distinct ectodomains for the target chain and protease chain, variables #7–9 and #11 and any reactions involving these variables do not occur. For VEGF-MESA, variables that contain VEGF and reactions that involve VEGF do not occur intracellularly. Thus, of the 44 possible receptor variables among two MESA in two cellular compartments (11 x 2 x 2), 28 can occur for the case of VEGF-MESA and Rap-MESA. Concentration is expressed in units that are arbitrary but comparable between chains.

Table M5: MESA receptor variables.

#	Variable	Attributes			
		monomer vs. dimer	without vs. with ligand	Target chains: cleaved vs. not	Number of bound TFs
1	T	monomer	without	not cleaved	1
2	X	monomer	without	cleaved	0
3	P	monomer	without	n/a	0
4	TL	monomer	with	not cleaved	1
5	XL	monomer	with	cleaved	0
6	PL	monomer	with	n/a	0
7	TLT	dimer	with	2 not cleaved	2
8	TLX	dimer	with	1 cleaved, 1 not cleaved	1
9	XLX	dimer	with	2 cleaved	0
10	XLP	dimer	with	cleaved	0
11	PLP	dimer	with	n/a	0

B. Parameter estimates

Parameter values were estimated by a Sobol sweep to explore the high-dimensional parameter space, followed by a custom script for a genetic algorithm with generations of multi-objective scoring, culling, repopulation, and mutation (**Table M6**). Units are concentration in arbitrary units (U) and time in hours (h). The first three parameters were fitted based on data without ligand, and yielded a family of parameter sets that described the data similarly. The next three parameters were fitted based on data with one or both ligands, and compared to without ligand, in combination with the family of the first three parameters.

Table M6: Parameter estimates obtained after calibrating the MESA model.

#	Parameter	Estimate	Units	Description
1	ksynM	0.116	n/a	Synthesis of receptors
2	kc	0.0538	$U^{-1} h^{-1}$	Enzymatic cleavage from transient encounters between chains
3	kdegT	0.280	h^{-1}	Degradation of target chain
4	kL1	0.909	h^{-1}	VEGF-MESA ligand-binding
5	kL2	0.341	h^{-1}	Rap-MESA ligand-binding
6	kac	0.703	$U^{-1} h^{-1}$	Chain dimerization (and enzymatic cleavage, if applicable)

C. Reactions

The MESA model specifies 28 reaction categories. In the naming, numbers 1 and 2 indicate species for VEGF-MESA-tTA and Rap-MESA-Gal4, respectively. Reactions at the plasma membrane do not have the *ild* multiplier but are otherwise equivalent to reactions that are intracellular. The cartoon illustrates differences for *ild* and *ecd* between the two MESA receptors (**Figure M8**).

ild Intracellular ligand diffusion

*ild*1 0 for VEGF-MESA-tTA, because VEGF cannot diffuse into the cell

*ild*2 1 for Rap-MESA-Gal4, because rapamycin can diffuse into the cell

ecd Extracellular domain dimerization

*ecd*1 1 for VEGF-MESA-tTA, because chains can potentially homodimerize with a ligand

*ecd*2 0 for Rap-MESA-Gal4, because chains cannot homodimerize with a ligand

pcs Enzymatic cleavage events, based on recognition of the cleavage sequence by the protease. In a hypothetical scenario without signaling crosstalk (i.e., MESA that are more orthogonal), *pcs*12 and *pcs*21 would both be zero. Given the current experimental implementation with the same protease and cleavage sequence, in which cross-cleavage events can in principle contribute to non-ligand-mediated signaling, these variables take a value of one.

*pcs*11 1 for VEGF-PC to VEGF-TC-tTA

*pcs*12 1 for VEGF-PC to Rap-TC-Gal4

*pcs*21 1 for Rap-PC to VEGF-TC-tTA

*pcs*22 1 for Rap-PC to Rap-TC-Gal4

The constants τ_{au1} and τ_{au2} are the time of treatment with VEGF and Rap, respectively, which occurs at 12 h post-transfection. Therefore, reactions with ligands and ligand-bound chains can occur only after 12 h. The Heaviside step function describes this change upon ligand treatment and is denoted by *u*.

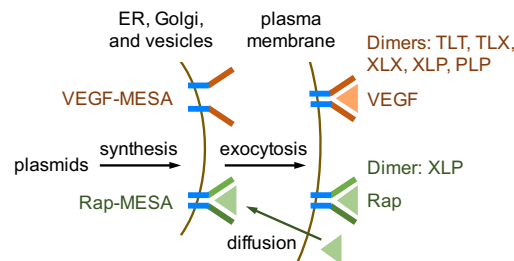


Figure M8: Intracellular ligand diffusion and ECD dimerization. VEGF-MESA and Rap-MESA have differences in ligand-inducible signaling.

Intracellular reactions between chains and ligands:

<u>1) T + L → TL</u>								
ild1			* kL1	* T1	* u(t-tauL1)			
	ild2		* kL2	* T2	* u(t-tauL2)			
<u>2) X + L → XL</u>								
ild1			* kL1	* X1	* u(t-tauL1)			
	ild2		* kL2	* X2	* u(t-tauL2)			
<u>3) P + L → PL</u>								
ild1			* kL1	* P1	* u(t-tauL1)			
	ild2		* kL2	* P2	* u(t-tauL2)			
<u>4) T + P → X + P + F</u>								
		pcs11	* kc	* T1	* P1			
		pcs12	* kc	* T1	* P2			
		pcs21	* kc	* T2	* P1			
		pcs22	* kc	* T2	* P2			
<u>5) T + TL → TLT</u>								
ild1		* ecd1		* ka1	* T1	* T1L1		
	ild2	* ecd2		* ka2	* T2	* T2L2		
<u>6) T + XL → TLX</u>								
ild1		* ecd1		* ka1	* T1	* X1L1		
	ild2	* ecd2		* ka2	* T2	* X2L2		
<u>7) T + PL → X + P + F</u>								
ild1			* pcs11	* kc	* T1	* P1L1		
	ild2		* pcs12	* kc	* T1	* P2L2		
ild1			* pcs21	* kc	* T2	* P1L1		
	ild2		* pcs22	* kc	* T2	* P2L2		
<u>8) T + PL → XLP + F</u>								
ild1			* pcs11	* kac1	* T1	* P1L1		
	ild2		* pcs22	* kac2	* T2	* P2L2		
<u>9) T + XLP → X + XLP + F</u>								
ild1			* pcs11	* kc	* T1	* X1L1P1		
	ild2		* pcs12	* kc	* T1	* X2L2P2		
ild1			* pcs21	* kc	* T2	* X1L1P1		
	ild2		* pcs22	* kc	* T2	* X2L2P2		
<u>10) T + PLP → X + PLP + F</u>								
ild1		* ecd1		* pcs11	* kc	* T1	* P1L1P1	
	ild2	* ecd2		* pcs12	* kc	* T1	* P2L2P2	
ild1		* ecd1		* pcs21	* kc	* T2	* P1L1P1	
	ild2	* ecd2		* pcs22	* kc	* T2	* P2L2P2	
<u>11) X + TL → TLX</u>								
ild1		* ecd1		* ka1	* X1	* T1L1		
	ild2	* ecd2		* ka2	* X2	* T2L2		
<u>12) X + XL → XLX</u>								
ild1		* ecd1		* ka1	* X1	* X1L1		
	ild2	* ecd2		* ka2	* X2	* X2L2		
<u>13) X + PL → XLP</u>								
ild1			* ka1	* X1	* P1L1			
	ild2		* ka2	* X2	* P2L2			
<u>14) P + TL → P + XL + F</u>								
ild1			* pcs11	* kc	* P1	* T1L1		
ild1			* pcs12	* kc	* P2	* T1L1		
	ild2		* pcs21	* kc	* P1	* T2L2		
	ild2		* pcs22	* kc	* P2	* T2L2		
<u>15) P + TL → XLP + F</u>								
ild1			* pcs11	* kac1	* P1	* T1L1		
	ild2		* pcs22	* kac2	* P2	* T2L2		

16) $P + XL \rightarrow XLP$

ild1			* ka1	* P1	* X1L1
	ild2		* ka2	* P2	* X2L2

17) $P + PL \rightarrow PLP$

ild1	* ecd1		* ka1	* P1	* P1L1
	ild2	* ecd2	* ka2	* P2	* P2L2

18) $P + TLT \rightarrow P + TLX + F$

ild1	* ecd1	* pcs11	* kc	* P1	* T1L1T1
ild1	* ecd1	* pcs12	* kc	* P2	* T1L1T1
	ild2	* ecd2	* pcs21	* P1	* T2L2T2
	ild2	* ecd2	* pcs22	* P2	* T2L2T2

19) $P + TLX \rightarrow P + XLX + F$

ild1	* ecd1	* pcs11	* kc	* P1	* T1L1X1
ild1	* ecd1	* pcs12	* kc	* P2	* T1L1X1
	ild2	* ecd2	* pcs21	* P1	* T2L2X2
	ild2	* ecd2	* pcs22	* P2	* T2L2X2

20) $TL + PL \rightarrow XL + PL + F$

ild1		* pcs11	* kc	* T1L1	* P1L1
ild1 * ild2		* pcs12	* kc	* T1L1	* P2L2
ild1 * ild2		* pcs21	* kc	* T2L2	* P1L1
	ild2	* pcs22	* kc	* T2L2	* P2L2

21) $TL + XLP \rightarrow XL + XLP + F$

ild1		* pcs11	* kc	* T1L1	* X1L1P1
ild1 * ild2		* pcs12	* kc	* T1L1	* X2L2P2
ild1 * ild2		* pcs21	* kc	* T2L2	* X1L1P1
	ild2	* pcs22	* kc	* T2L2	* X2L2P2

22) $TL + PLP \rightarrow XL + PLP + F$

ild1	* ecd1	* pcs11	* kc	* T1L1	* P1L1P1
ild1 * ild2	* ecd2	* pcs12	* kc	* T1L1	* P2L2P2
ild1 * ild2 * ecd1		* pcs21	* kc	* T2L2	* P1L1P1
	ild2	* ecd2	* pcs22	* T2L2	* P2L2P2

23) $PL + TLT \rightarrow PL + TLX + F$

ild1	* ecd1	* pcs11	* kc	* P1L1	* T1L1T1
ild1 * ild2 * ecd1		* pcs12	* kc	* P2L2	* T1L1T1
ild1 * ild2	* ecd2	* pcs21	* kc	* P1L1	* T2L2T2
	ild2	* ecd2	* pcs22	* P2L2	* T2L2T2

24) $PL + TLX \rightarrow PL + XLX + F$

ild1	* ecd1	* pcs11	* kc	* P1L1	* T1L1X1
ild1 * ild2 * ecd1		* pcs12	* kc	* P2L2	* T1L1X1
ild1 * ild2	* ecd2	* pcs21	* kc	* P1L1	* T2L2X2
	ild2	* ecd2	* pcs22	* P2L2	* T2L2X2

25) $TLT + XLP \rightarrow TLX + XLP + F$

ild1	* ecd1	* pcs11	* kc1c1	* T1L1T1	* X1L1P1
ild1 * ild2 * ecd1		* pcs12	* kc1c2	* T1L1T1	* X2L2P2
ild1 * ild2	* ecd2	* pcs21	* kc2c1	* T2L2T2	* X1L1P1
	ild2	* ecd2	* pcs22	* T2L2T2	* X2L2P2

26) $TLT + PLP \rightarrow TLX + PLP + F$

ild1	* ecd1	* pcs11	* kc1c1	* T1L1T1	* P1L1P1
ild1 * ild2 * ecd1	* ecd2	* pcs12	* kc1c2	* T1L1T1	* P2L2P2
ild1 * ild2 * ecd1	* ecd2	* pcs21	* kc2c1	* T2L2T2	* P1L1P1
	ild2	* ecd2	* pcs22	* T2L2T2	* P2L2P2

27) $TLX + XLP \rightarrow XLX + XLP + F$

ild1	* ecd1	* pcs11	* kc1c1	* T1L1X1	* X1L1P1
ild1 * ild2 * ecd1		* pcs12	* kc1c2	* T1L1X1	* X2L2P2
ild1 * ild2	* ecd2	* pcs21	* kc2c1	* T2L2X2	* X1L1P1
	ild2	* ecd2	* pcs22	* T2L2X2	* X2L2P2

28) $TLX + PLP \rightarrow XLX + PLP + F$

ild1	* ecd1	* pcs11	* kc1c1	* T1L1X1	* P1L1P1
ild1 * ild2 * ecd1	* ecd2	* pcs12	* kc1c2	* T1L1X1	* P2L2P2
ild1 * ild2 * ecd1	* ecd2	* pcs21	* kc2c1	* T2L2X2	* P1L1P1
	ild2	* ecd2	* pcs22	* T2L2X2	* P2L2P2

D. Fixed parameters

Receptors and TFs

First-order transport from inside the cell to the plasma membrane via exocytosis (h^{-1}). This value was chosen to be slightly lower than typical values reported in the literature for native proteins (Hirschberg et al., 1998), but may account for potential delays associated with synthesizing and exocytosing atypically large amounts of functional exogenous receptors. Each receptor is assumed to be exocytosed similarly.

k_{sec}	= 0.4	
k_{secT}	= k_{sec}	Target chains and ligand-bound target chains
k_{secX}	= k_{sec}	Cleaved target chains and ligand-bound cleaved target chains
k_{secP}	= k_{sec}	Protease chains and ligand-bound protease chains
k_{secTT}	= k_{sec}	Target chain homodimers
k_{secTX}	= k_{sec}	Target chain-cleaved target chain heterodimers
k_{secXX}	= k_{sec}	Cleaved target chain homodimers
k_{secXP}	= k_{sec}	Cleaved target chain-protease chain heterodimers
k_{secPP}	= k_{sec}	Protease chain homodimers

First-order degradation of soluble TFs (h^{-1}) is rapid (di Bernardo et al., 2011). For simplification, both TFs are assigned the same rate constant.

k_{degF1}	= 2	tTA.
k_{degF2}	= 2	Gal4.

First-order degradation of receptor chains (h^{-1}). Surface staining experiments (not shown) indicated that average protease chain expression was consistently lower (about half) compared to average target chain expression across a range of transfection doses.

k_{degX}	= k_{degT}
k_{degP}	= $k_{degT} / 0.6$
k_{degTT}	= k_{degT}
k_{degTX}	= k_{degT}
k_{degXX}	= k_{degT}
k_{degXP}	= $k_{degT} / 0.6$
k_{degPP}	= $k_{degT} / 0.6$

Receptor binding to a ligand-bound receptor.

k_{a1}	= k_{ac}	VEGF-MESA binds to a VEGF-bound chain.
k_{a2}	= k_{ac}	Rap-MESA binds to a Rap-bound chain.
k_{ac1}	= k_{ac}	VEGF-MESA binds to a VEGF-bound chain, and a cleavage event follows.
k_{ac2}	= k_{ac}	Rap-MESA binds to a Rap-bound chain, and a cleavage event follows.

Cleavage of a ligand-bound receptor dimer by another ligand-bound receptor dimer.

k_{c1c1}	= k_c	Cleavage of a VEGF-bound dimer by another VEGF-bound dimer.
k_{c1c2}	= k_c	Cleavage of a VEGF-bound dimer by a Rap-bound dimer.
k_{c2c1}	= k_c	Cleavage of a Rap-bound dimer by a VEGF-bound dimer.
k_{c2c2}	= k_c	Cleavage of a Rap-bound dimer by another Rap-bound dimer.

Synthesis of receptors or soluble TFs. One arbitrary unit of concentration per hour, per amount of plasmid received by a mean-transfected cell, per μg of transfected plasmid. Note: for receptor expression, k_{syn} is multiplied by the free parameter k_{synM} .

$$k_{syn} = 1$$

Reporter expression

(Arbitrary units of concentration for reporter expression are distinct from those for the other variables.)

$k_{tx} = 1$	Max. rate of transcription of Reporter RNA ($U h^{-1}$). Assigned a unit value of one.
$k_{t1} = 1$	Translation of Reporter protein (h^{-1}). Assigned a unit value of one.
$k_{degRepR} = 2.3$	Degradation of Reporter RNA (h^{-1}); short half-life (Siciliano et al., 2011).
$k_{degRepP} = 0.054$	Degradation of Reporter protein (h^{-1}); long half-life (Siciliano et al., 2011).

Intercellular variation

The population matrix Z (dimensions: 200 cells x 5 plasmids) has unitless multipliers for the synthesis terms in the model. Variation among cells due to transfection, transcription, and translation is incorporated by the rows, and covariation among cotransfected plasmids is incorporated by the columns.

$Z_{T1} = Z(c, 1)$	VEGF-MESA target chain
$Z_{F1} = Z(c, 1)$	Soluble tTA
$Z_{T2} = Z(c, 2)$	Rap-MESA target chain
$Z_{F2} = Z(c, 2)$	Soluble Gal4
$Z_{Rep} = Z(c, 3)$	Inducible reporters: tTA-inducible, Rap-inducible, H1 hybrid, or H2 hybrid
$Z_{P1} = Z(c, 4)$	VEGF-MESA protease chain
$Z_{P2} = Z(c, 5)$	Rap-MESA protease chain

E. Conditions

The types of conditions in **Table M7** were considered in the experiments and simulations. For each row, doses of transfected components can be varied. The dose of each ligand was held constant.

Table M7: Conditions for experiments and simulations

#	Soluble TF		MESA				Ligand	
	tTA	Gal4	TC _V	PC _V	TC _R	PC _R	VEGF	Rap
1	x							
2		x						
3	x	x						
4			x	x				
5			x	x			x	
6		x	x	x				
7		x	x	x			x	
8					x	x		
9					x	x		x
10	x				x	x		
11	x				x	x		x
12			x	x	x	x		
13			x	x	x	x	x	
14			x	x	x	x		x
15			x	x	x	x	x	x

Conditions correspond to the following experimental figures:

#1-3 for Figure 1

#4-11 for Figure 2a

#12-15 for Figure 2b

F. TFs and reporters

ODE for soluble tTA (s = intracellular compartment; m = plasma membrane compartment)

```

d tTA / dt =
-
+           ZF1 * ksyn * dF1
+           kdegF1 * tTA
+           pcs11 * kc * T1s * P1s #rxn4
+           pcs11 * kc * T1m * P1m
+           pcs12 * kc * T1s * P2s
+           pcs12 * kc * T1m * P2m
+   ild1    * pcs11 * kc * T1s * P1L1s #rxn7
+           pcs11 * kc * T1m * P1L1m
+           ild2    * pcs12 * kc * T1s * P2L2s
+           pcs12 * kc * T1m * P2L2m
+   ild1    * pcs11 * kac1 * T1s * P1L1s #rxn8
+           pcs11 * kac1 * T1m * P1L1m
+   ild1    * pcs11 * kc * T1s * X1L1P1s #rxn9
+           pcs11 * kc * T1m * X1L1P1m
+           ild2    * pcs12 * kc * T1s * X2L2P2s
+           pcs12 * kc * T1m * X2L2P2m
+   ild1    * ecd1    * pcs11 * kc * T1s * P1L1P1s #rxn10
+           ecd1    * pcs11 * kc * T1m * P1L1P1m
+           ild2    * ecd2    * pcs12 * kc * T1s * P2L2P2s
+           ecd2    * pcs12 * kc * T1m * P2L2P2m
+   ild1    * ecd1    * pcs11 * kc * P1s * T1L1s #rxn14
+           ecd1    * pcs11 * kc * P1m * T1L1m
+   ild1    * ecd1    * pcs12 * kc * P2s * T1L1s
+           ecd1    * pcs12 * kc * P2m * T1L1m
+   ild1    * ecd1    * pcs11 * kac1 * P1s * T1L1s #rxn15
+           ecd1    * pcs11 * kac1 * P1m * T1L1m
+   ild1    * ecd1    * pcs11 * kc * P1s * T1L1T1s #rxn18
+           ecd1    * pcs11 * kc * P1m * T1L1T1m
+   ild1    * ecd1    * pcs12 * kc * P2s * T1L1T1s
+           ecd1    * pcs12 * kc * P2m * T1L1T1m
+   ild1    * ecd1    * pcs11 * kc * P1s * T1L1X1s #rxn19
+           ecd1    * pcs11 * kc * P1m * T1L1X1m
+   ild1    * ecd1    * pcs12 * kc * P2s * T1L1X1s
+           ecd1    * pcs12 * kc * P2m * T1L1X1m
+   ild1    * ecd1    * pcs11 * kc * T1L1s * P1L1s #rxn20
+           ecd1    * pcs11 * kc * T1L1m * P1L1m
+   ild1 * ild2    * pcs12 * kc * T1L1s * P2L2s
+           ecd1    * pcs12 * kc * T1L1m * P2L2m
+   ild1    * ecd1    * pcs11 * kc * T1L1s * X1L1P1s #rxn21
+           ecd1    * pcs11 * kc * T1L1m * X1L1P1m
+   ild1 * ild2    * ecd1    * pcs12 * kc * T1L1s * X2L2P2s
+           ecd1    * pcs12 * kc * T1L1m * X2L2P2m
+   ild1    * ecd1    * pcs11 * kc * T1L1s * P1L1P1s #rxn22
+           ecd1    * pcs11 * kc * T1L1m * P1L1P1m
+   ild1 * ild2    * ecd2    * pcs12 * kc * T1L1s * P2L2P2s
+           ecd2    * pcs12 * kc * T1L1m * P2L2P2m
+   ild1    * ecd1    * pcs11 * kc * P1L1s * T1L1T1s #rxn23
+           ecd1    * pcs11 * kc * P1L1m * T1L1T1m
+   ild1 * ild2    * ecd1    * pcs12 * kc * P2L2s * T1L1T1s
+           ecd1    * pcs12 * kc * P2L2m * T1L1T1m
+   ild1    * ecd1    * pcs11 * kc * P1L1s * T1L1X1s #rxn24
+           ecd1    * pcs11 * kc * P1L1m * T1L1X1m
+   ild1 * ild2    * ecd1    * pcs12 * kc * P2L2s * T1L1X1s
+           ecd1    * pcs12 * kc * P2L2m * T1L1X1m
+   ild1    * ecd1    * pcs11 * kc1c1 * T1L1T1s * X1L1P1s #rxn25
+           ecd1    * pcs11 * kc1c1 * T1L1T1m * X1L1P1m
+   ild1 * ild2    * ecd1    * pcs12 * kc1c2 * T1L1T1s * X2L2P2s
+           ecd1    * pcs12 * kc1c2 * T1L1T1m * X2L2P2m
+   ild1    * ecd1    * pcs11 * kc1c1 * T1L1T1s * P1L1P1s #rxn26
+           ecd1    * pcs11 * kc1c1 * T1L1T1m * P1L1P1m
+   ild1 * ild2    * ecd1 * ecd2 * pcs12 * kc1c2 * T1L1T1s * P2L2P2s
+           ecd2    * pcs12 * kc1c2 * T1L1T1m * P2L2P2m
+   ild1    * ecd1    * pcs11 * kc1c1 * T1L1X1s * X1L1P1s #rxn27
+           ecd1    * pcs11 * kc1c1 * T1L1X1m * X1L1P1m
+   ild1 * ild2    * ecd1    * pcs12 * kc1c2 * T1L1X1s * X2L2P2s
+           ecd1    * pcs12 * kc1c2 * T1L1X1m * X2L2P2m
+   ild1    * ecd1    * pcs11 * kc1c1 * T1L1X1s * P1L1P1s #rxn28
+           ecd1    * pcs11 * kc1c1 * T1L1X1m * P1L1P1m
+   ild1 * ild2    * ecd1 * ecd2 * pcs12 * kc1c2 * T1L1X1s * P2L2P2s
+           ecd2    * pcs12 * kc1c2 * T1L1X1m * P2L2P2m

```

ODE for soluble Gal4 (s = intracellular compartment; m = plasma membrane compartment)

```

d Gal4 / dt =
      ZF2 * ksyn * dF2
-      kdegF2 * Gal4
+      pcs21 * kc * T2s * P1s #rxn4
+      pcs21 * kc * T2m * P1m
+      pcs22 * kc * T2s * P2s
+      pcs22 * kc * T2m * P2m
+ ild1      * pcs21 * kc * T2s * P1L1s #rxn7
+      pcs21 * kc * T2m * P1L1m
+      ild2      * pcs22 * kc * T2s * P2L2s
+      pcs22 * kc * T2m * P2L2m
+      ild2      * pcs22 * kac2 * T2s * P2L2s #rxn8
+      pcs22 * kac2 * T2m * P2L2m
+ ild1      * pcs21 * kc * T2s * X1L1P1s #rxn9
+      pcs21 * kc * T2m * X1L1P1m
+      ild2      * pcs22 * kc * T2s * X2L2P2s
+      pcs22 * kc * T2m * X2L2P2m
+ ild1      * ecd1      * pcs21 * kc * T2s * P1L1P1s #rxn10
+      ecd1      * pcs21 * kc * T2m * P1L1P1m
+      ild2      * ecd2      * pcs22 * kc * T2s * P2L2P2s
+      ecd2      * pcs22 * kc * T2m * P2L2P2m
+      ild2      * pcs21 * kc * P1s * T2L2s #rxn14
+      pcs21 * kc * P1m * T2L2m
+      ild2      * pcs22 * kc * P2s * T2L2s
+      pcs22 * kc * P2m * T2L2m
+      ild2      * pcs22 * kac2 * P2s * T2L2s #rxn15
+      pcs22 * kac2 * P2m * T2L2m
+      ild2      * ecd2 * pcs21 * kc * P1s * T2L2T2s #rxn18
+      ecd2 * pcs21 * kc * P1m * T2L2T2m
+      ild2      * ecd2 * pcs22 * kc * P2s * T2L2T2s
+      ecd2 * pcs22 * kc * P2m * T2L2T2m
+      ild2      * ecd2 * pcs21 * kc * P1s * T2L2X2s #rxn19
+      ecd2 * pcs21 * kc * P1m * T2L2X2m
+      ild2      * ecd2 * pcs22 * kc * P2s * T2L2X2s
+      ecd2 * pcs22 * kc * P2m * T2L2X2m
+ ild1 * ild2      * pcs21 * kc * T2L2s * P1L1s #rxn20
+      pcs21 * kc * T2L2m * P1L1m
+      ild2      * pcs22 * kc * T2L2s * P2L2s
+      pcs22 * kc * T2L2m * P2L2m
+ ild1 * ild2      * pcs21 * kc * T2L2s * X1L1P1s #rxn21
+      pcs21 * kc * T2L2m * X1L1P1m
+      ild2      * pcs22 * kc * T2L2s * X2L2P2s
+      pcs22 * kc * T2L2m * X2L2P2m
+ ild1 * ild2 * ecd1      * pcs21 * kc * T2L2s * P1L1P1s #rxn22
+      ecd1      * pcs21 * kc * T2L2m * P1L1P1m
+      ild2      * ecd2 * pcs22 * kc * T2L2s * P2L2P2s
+      ecd2 * pcs22 * kc * T2L2m * P2L2P2m
+ ild1 * ild2      * ecd2 * pcs21 * kc * P1L1s * T2L2T2s #rxn23
+      ecd2 * pcs21 * kc * P1L1m * T2L2T2m
+      ild2      * ecd2 * pcs22 * kc * P2L2s * T2L2T2s
+      ecd2 * pcs22 * kc * P2L2m * T2L2T2m
+ ild1 * ild2      * ecd2 * pcs21 * kc * P1L1s * T2L2X2s #rxn24
+      ecd2 * pcs21 * kc * P1L1m * T2L2X2m
+      ild2      * ecd2 * pcs22 * kc * P2L2s * T2L2X2s
+      ecd2 * pcs22 * kc * P2L2m * T2L2X2m
+ ild1 * ild2      * ecd2 * pcs21 * kc2c1 * T2L2T2s * X1L1P1s #rxn25
+      ecd2 * pcs21 * kc2c1 * T2L2T2m * X1L1P1m
+      ild2      * ecd2 * pcs22 * kc2c2 * T2L2T2s * X2L2P2s
+      ecd2 * pcs22 * kc2c2 * T2L2T2m * X2L2P2m
+ ild1 * ild2 * ecd1      * ecd2 * pcs21 * kc2c1 * T2L2T2s * P1L1P1s #rxn26
+      ecd1      * ecd2 * pcs21 * kc2c1 * T2L2T2m * P1L1P1m
+      ild2      * ecd2 * pcs22 * kc2c2 * T2L2T2s * P2L2P2s
+      ecd2 * pcs22 * kc2c2 * T2L2T2m * P2L2P2m
+ ild1 * ild2      * ecd2 * pcs21 * kc2c1 * T2L2X2s * X1L1P1s #rxn27
+      ecd2 * pcs21 * kc2c1 * T2L2X2m * X1L1P1m
+      ild2      * ecd2 * pcs22 * kc2c2 * T2L2X2s * X2L2P2s
+      ecd2 * pcs22 * kc2c2 * T2L2X2m * X2L2P2m
+ ild1 * ild2 * ecd1      * ecd2 * pcs21 * kc2c1 * T2L2X2s * P1L1P1s #rxn28
+      ecd1      * ecd2 * pcs21 * kc2c1 * T2L2X2m * P1L1P1m
+      ild2      * ecd2 * pcs22 * kc2c2 * T2L2X2s * P2L2P2s
+      ecd2 * pcs22 * kc2c2 * T2L2X2m * P2L2P2m

```

ODEs for reporter expression

tTA-inducible reporter

```
d RNA / dt =
  ZRep * ktx * tTA
  - kdegRepR * RNA

d Protein / dt =
  ktl * RNA
  - kdegRepP * Protein
```

Gal4-inducible reporter

```
d RNA / dt =
  ZRep * ktx * Gal4
  - kdegRepR * RNA

d Protein / dt =
  ktl * RNA
  - kdegRepP * Protein
```

H1 hybrid promoter reporter

```
d RNA / dt =
  ZRep * ktx * (wH1_T * tTA + wH1_G * Gal4 + wH1_TG * tTA * Gal4)
  / (1 + wH1_T * tTA + wH1_G * Gal4 + wH1_TG * tTA * Gal4)
  - kdegRepR * RNA

d Protein / dt =
  ktl * RNA
  - kdegRepP * Protein
```

H2 hybrid promoter reporter

```
d RNA / dt =
  ZRep * ktx * (wH2_T * tTA + wH2_G * Gal4 + wH2_TG * tTA * Gal4)
  / (1 + wH2_T * tTA + wH2_G * Gal4 + wH2_TG * tTA * Gal4)
  - kdegRepR * RNA

d Protein / dt =
  ktl * RNA
  - kdegRepP * Protein
```

V. MODEL PREDICTIONS

A. Dosing

Receptor doses for each MESA in combination with a soluble TF were examined for promoters H1 and H2 (**Figure M9**). Wet-lab experiments suggested that constitutively soluble TF (0.05 μg) generally had more influence on promoter activity than TF released from receptors. Therefore, during model development, the parameter $ksynM$ was introduced as a unitless multiplier for the rate of synthesis ($0 < ksynM < 1$) of receptors compared to soluble proteins. The estimate for $ksynM$ after calibration to the data was 0.116, indicating much lower synthesis for receptors. This difference explains in part why ligand-inducible signaling has a relatively modest effect in Figure 2a, and why, at low receptor doses, the F.D. remains near one.

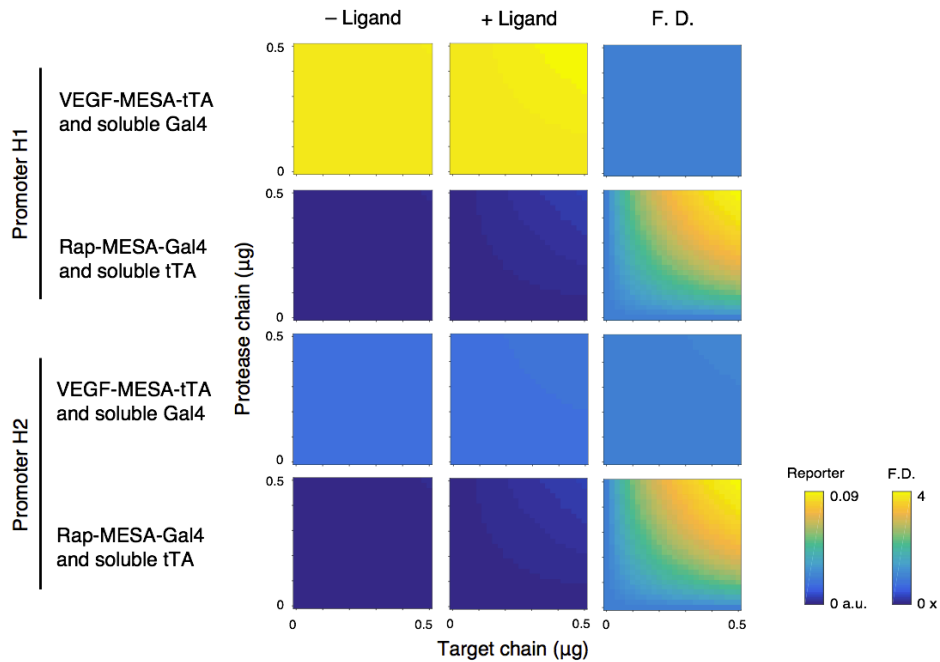


Figure M9: Reporter expression from hybrid promoters for each pair of receptor and soluble factor. Outcomes corresponding to experiments in Figure 2a are shown for the mean-transfected cell. Heatmaps show reporter expression from each hybrid promoter, for each pair of receptor and soluble TF, for a constant TF dose (0.05 μg plasmid) and different TC and PC doses, with and without ligand. (Color scaling is distinct for reporter expression in a.u. and for unitless F.D.)

We examined the dynamics of reporter expression for different receptor and promoter implementations (**Figure M10**). A consistent trend for the single-TF promoters and H1 promoter is that reporter expression increases as either chain dose is increased, as well as with ligand treatment. For multiplexed receptors, while non-ligand-mediated signaling increases due to crosstalk, reporter expression from each single-TF promoter remains ligand-inducible. However, for the hybrid promoter, a wide range of TC and PC doses yield a relatively low two-ligand inducible reporter expression compared to either ligand individually or no ligand. The analysis indicates that the amounts of TFs that can be released from receptors is less than the amount required to synergistically activate the promoter.

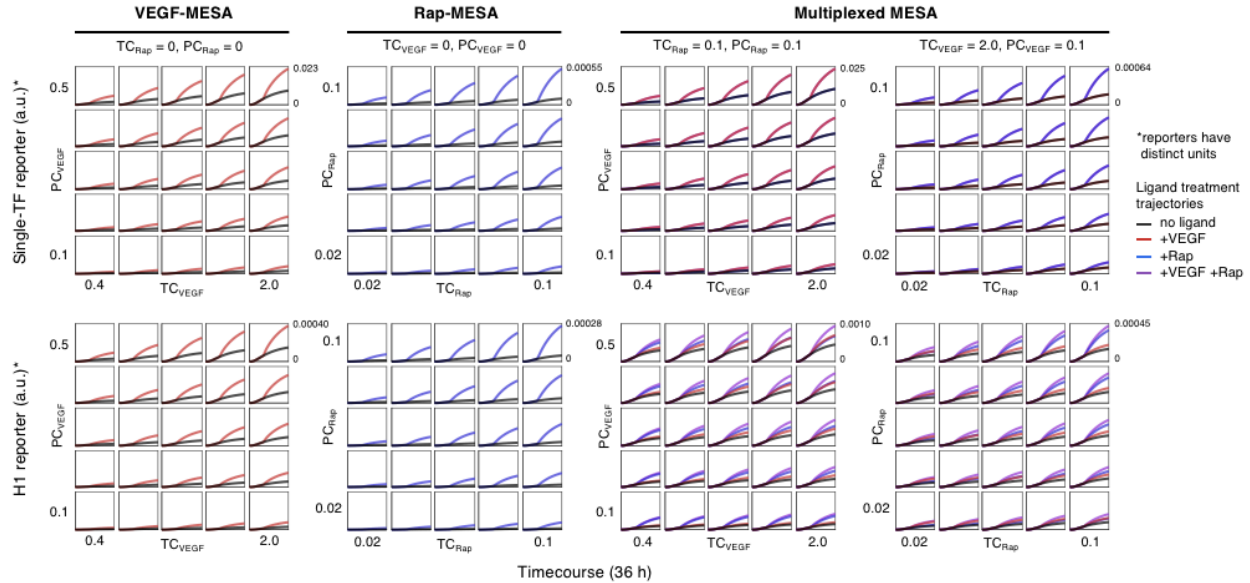


Figure M10: Timecourse trajectories. Simulations show predicted timecourse reporter trajectories for single-TF inducible promoters and the H1 promoter, for different TC and PC doses, for single and multiplexed MESA, with and without each ligand, for the mean-transfected cell. (Y-axis units for arbitrary concentration are different between the single-TF promoters and the H1 promoter.)

We analyzed individual MESA with and without ligand. The results suggest that the way in which ligand-inducible fold-difference (F.D.) is assessed experimentally—as a ratio of population means—may lead to interpretations of performance outcomes that differ from those in individual cells (**Figure M11**). However, true single-cell F.D. outcomes are not directly measurable in experiments because each cell is treated with *or* without ligand, not both; thus, such precise outcomes will for practical reasons remain unobservable.

We also investigated an *all-in-one* plasmid scenario, in which genes are cloned onto the same plasmid. While ligand-inducible expression is predicted to increase compared to with separate plasmids, there is a trade-off of higher background signaling, and so the overall performance (F.D.) remains similar.

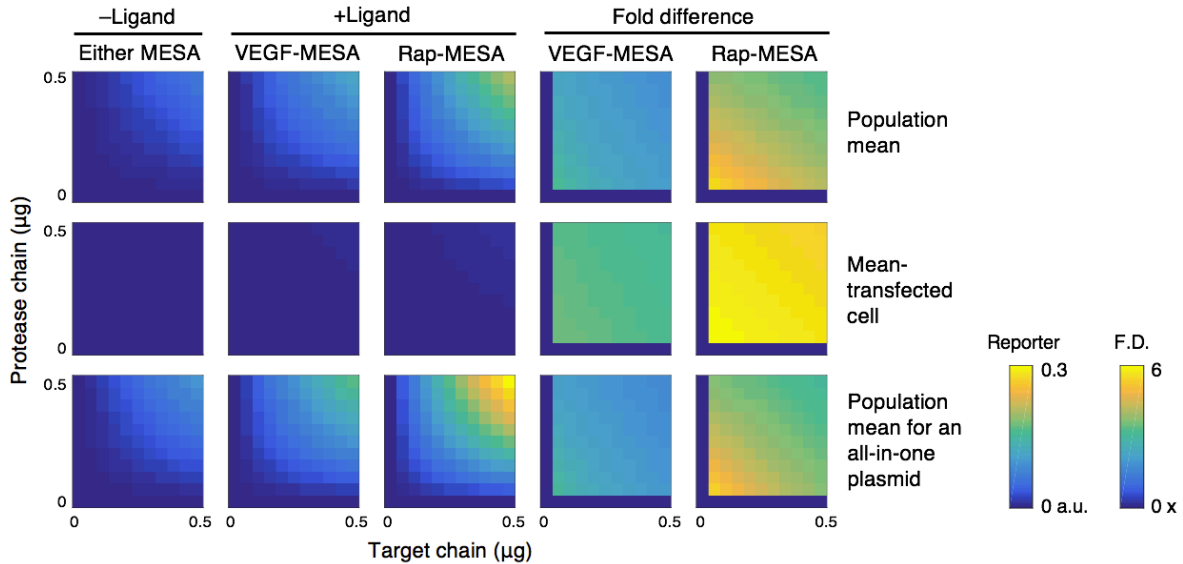


Figure M11: Ligand-inducibility for individual MESA. Expression of a reporter driven by a single-TF inducible promoter is shown for single-receptor TC and PC doses, with and without ligand, for the population mean, mean-transfected cell, and population mean in a scenario where genes are cloned onto one plasmid and within-cell covariance is zero. VEGF-MESA and Rap-MESA are shown, and in the absence of ligand their outcomes are equivalent. (Color scaling is distinct for expression in a.u. and for unitless F.D.)

B. Time points

We examined the choice of time points for ligand treatment and reporter measurement (**Figure M12**). Although adding ligands earlier and conducting flow cytometry later may increase the measured F.D., these effects are predicted to be modest, especially for two-ligand induced F.D. with respect to either ligand individually. Characterization from the experimentally implemented time points (coordinate [12, 24] in the figure) approaches the highest attainable F.D. Therefore, obtaining new experimental measurements at different time points would not affect the main conclusions about receptor performance.

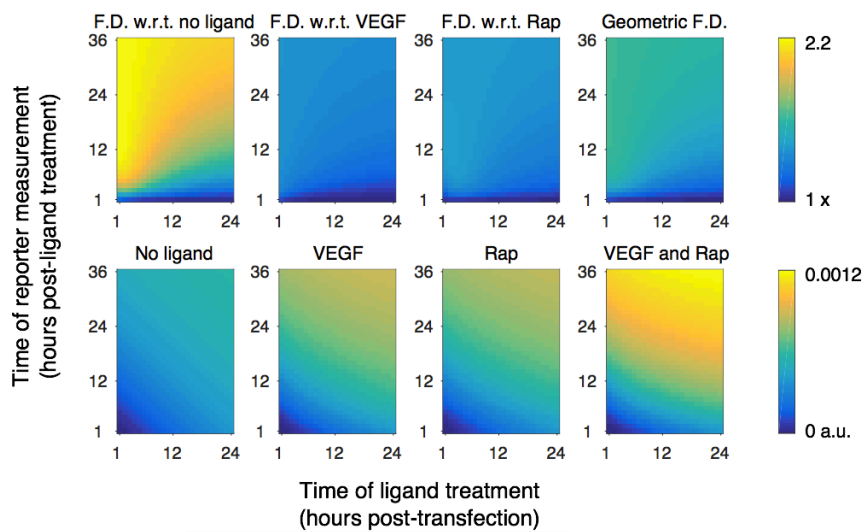


Figure M12: Effect of the time of ligand treatment and the time of measurement on H1 reporter expression and F.D. for multiplexed MESA. Time of ligand treatment was varied between 1 to 24 h post-transfection, and time of measurement was varied between 1 to 36 h post-ligand treatment. Reporter expression with both, either, or neither ligand was determined for the mean-transfected cell, for one dose ($TC_{VEGF} = 2$, $PC_{VEGF} = 0.5$, $TC_{Rap} = 0.1$, $PC_{Rap} = 0.1 \mu\text{g}$). Two-ligand-inducible F.D. was determined with respect to either and neither ligand. As an additional metric, we show geometric F.D.: two-ligand induced expression divided by the third root of the product of expression in the other three cases. (Color scaling is distinct for expression in a.u. and for unitless F.D.)

C. Promoters

Since changes to promoter responsiveness and synergy conferred improved AND gate performance in Figure 6, we examined the same types of changes with larger effect-magnitudes (**Figure M13**). The best possible outcomes resembled the previous ones, indicating that for a given MESA pairing such as with the current receptors, improvements that can be conferred through promoter engineering alone are inherently bounded. For a hypothetical promoter that is already highly responsive or synergistic, further increases to responsiveness or synergy have diminishing returns.

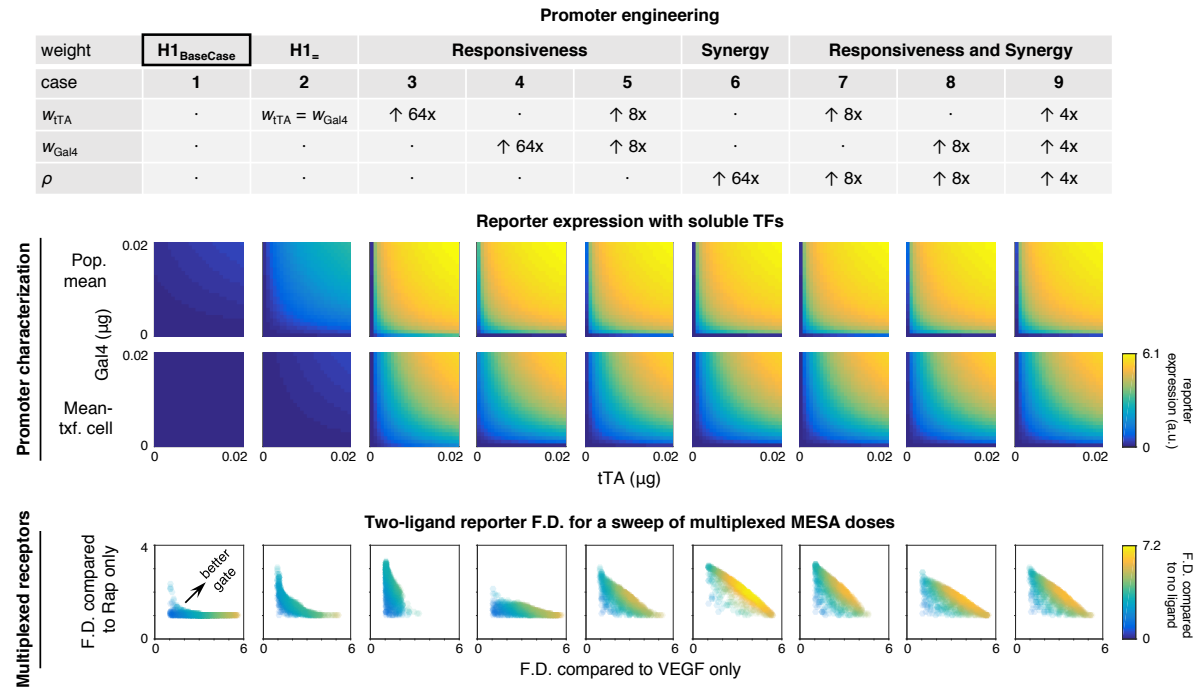


Figure M13: Promoter modifications with large effect-magnitudes have diminishing returns on AND gate performance improvement. A panel of promoters that vary in responsiveness to each TF and in synergy were produced, corresponding to promoter cases in Figure 6 but with greater effect-magnitudes. For example, responsiveness to tTA in case #3 is increased by 64x here compared to 16x. Panels show the TF dose landscapes and reporter F.D. (Color scaling is distinct for expression in a.u. and for unitless F.D.)

VI. REFERENCES

di Bernardo, D., Marucci, L., Menolascina, F., and Siciliano, V. (2011). Predicting synthetic gene networks. In *Synthetic gene networks: methods and protocols*, W. Weber, and M. Fussenegger, eds. (Springer Science+Business Media), pp. 57-81.

Hirschberg, K., Miller, C.M., Ellenberg, J., Presley, J.F., Siggia, E.D., Phair, R.D., and Lippincott-Schwartz, J. (1998). Kinetic analysis of secretory protein traffic and characterization of Golgi to plasma membrane transport intermediates in living cells. *J Cell Biol* 143, 1485-1503.

Siciliano, V., Menolascina, F., Marucci, L., Fracassi, C., Garzilli, I., Moretti, M.N., and di Bernardo, D. (2011). Construction and modelling of an inducible positive feedback loop stably integrated in a mammalian cell-line. *PLoS Comp Biol* 7, e1002074.

Sobol, I.M. (1976). Uniformly distributed sequences with an additional uniform property. *USSR Comp Math Math+* 16, 1332-1337.